



# Soil moisture controls on phenology and productivity in a semi-arid critical zone☆



James Cleverly<sup>a,b,\*</sup>, Derek Eamus<sup>a,b</sup>, Natalia Restrepo Coupe<sup>a,c</sup>, Chao Chen<sup>d</sup>, Wouter Maes<sup>a,c,1</sup>, Longhui Li<sup>a</sup>, Ralph Faux<sup>a</sup>, Nadia S. Santini<sup>a</sup>, Rizwana Rumman<sup>a</sup>, Qiang Yu<sup>a</sup>, Alfredo Huete<sup>a,c</sup>

<sup>a</sup> School of Life Sciences, University of Technology Sydney, PO Box 123, Broadway, NSW 2007, Australia

<sup>b</sup> Australian SuperSite Network, University of Technology Sydney, PO Box 123, Broadway, NSW 2007, Australia

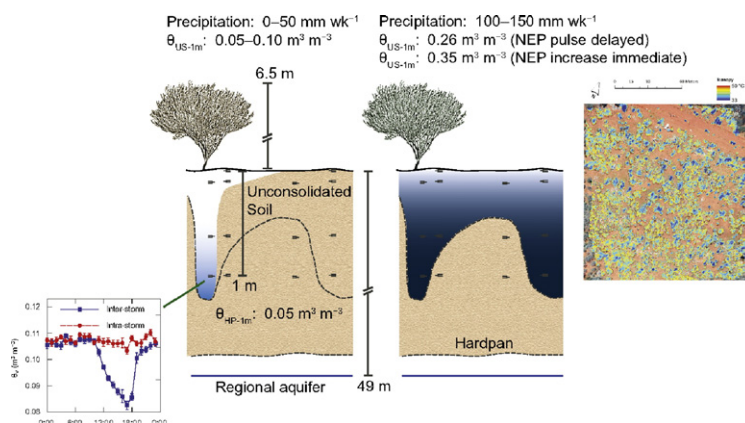
<sup>c</sup> Plant Functional Biology and Climate Change Cluster, University of Technology Sydney, Australia

<sup>d</sup> CSIRO Agriculture Flagship, PMB 5, PO Wembley, WA 6913, Australia

## HIGHLIGHTS

- Carry-over of soil moisture enhances ecosystem responses to precipitation.
- Excessive heat and atmospheric demand promote delayed productivity.
- Phenological delay was disabled following extreme precipitation ( $> 120 \text{ mm wk}^{-1}$ ).
- Hydraulic lift was proposed as a mechanism to maintain surface root function.

## GRAPHICAL ABSTRACT



## ARTICLE INFO

### Article history:

Received 27 December 2015

Received in revised form 19 May 2016

Accepted 19 May 2016

Available online 27 May 2016

Editor: D. Barcelo

### Keywords:

Ecohydrology

Resilience

Soil moisture carry-over

## ABSTRACT

The Earth's Critical Zone, where physical, chemical and biological systems interact, extends from the top of the canopy to the underlying bedrock. In this study, we investigated soil moisture controls on phenology and productivity of an *Acacia* woodland in semi-arid central Australia. Situated on an extensive sand plain with negligible runoff and drainage, the carry-over of soil moisture content ( $\theta$ ) in the rhizosphere enabled the delay of phenology and productivity across seasons, until conditions were favourable for transpiration of that water to prevent overheating in the canopy. Storage of soil moisture near the surface (in the top few metres) was promoted by a siliceous hardpan. Pulsed recharge of  $\theta$  above the hardpan was rapid and depended upon precipitation amount: 150 mm storm<sup>-1</sup> resulted in saturation of  $\theta$  above the hardpan (i.e., formation of a temporary, discontinuous perched aquifer above the hardpan in unconsolidated soil) and immediate carbon uptake by the vegetation. During dry and inter-storm periods, we inferred the presence of hydraulic lift from soil storage above the hardpan to the surface due to (i) regular daily drawdown of  $\theta$  in the reservoir that accumulates above the hardpan in the

☆ Special issue: Landscape evolution and intensification in Australia: The Living Critical Zone perspective.

\* Corresponding author at: School of Life Sciences, University of Technology Sydney, PO Box 123, Broadway, NSW 2007, Australia.

E-mail address: [james.cleverly@uts.edu.au](mailto:james.cleverly@uts.edu.au) (J. Cleverly).

<sup>1</sup> Current address: Laboratory of Plant Ecology, Ghent University, Coupure Links, 653, 9000 Gent, Belgium.

Climate extremes  
Semi-arid woodland  
Evergreen Acacia

absence of drainage and evapotranspiration; (ii) the dimorphic root distribution wherein most roots were found in dry soil near the surface, but with significant root just above the hardpan; and (iii) synchronisation of phenology amongst trees and grasses in the dry season. We propose that hydraulic redistribution provides a small amount of moisture that maintains functioning of the shallow roots during long periods when the surface soil layer was dry, thereby enabling Mulga to maintain physiological activity without diminishing phenological and physiological responses to precipitation when conditions were favourable to promote canopy cooling.

© 2016 Elsevier B.V. All rights reserved.

## 1. Introduction

The generic term *critical zone* was first used in 1909 to describe the chemical interface between two mixing fluids (Tsakalotos, 1909; cited from Lin, 2010), and more recently it has been used in petroleum geology (for mineral bearing strata of the Bushveld complex; Ballhaus and Stumpfl, 1985), in cardiac physiology (Touboul et al., 1992), and for the root–soil interface (Ryan et al., 2001). Recently, the Earth's Critical Zone was defined to integrate the ecohydrology, climate and geology of the near-surface terrestrial environment, from the top of the vegetation through to the bottom of the aquifer (Lin, 2010; Banwart et al., 2011; Chorover et al., 2011; Lin, 2011). In this current paradigm, study of the Earth's Critical Zone often focuses on water as a unifying theme, through which soil moisture content ( $\theta$ ) is the medium that bridges biotic and abiotic processes by providing site memory and integrating climate and biological systems (Lin, 2010; Banwart et al., 2011; Lin, 2011).

Vegetation dynamics (e.g., productivity) are primarily constrained by low soil moisture availability in dryland regions of the world, thus knowledge of the spatial and temporal dynamics of  $\theta$  are crucial for understanding patterns and processes in dryland critical zones. Drylands include environments characterised by dry sub-humid, semi-arid, arid and hyper-arid climates, and their distribution covers 41% of global land area and is increasing (Reynolds et al., 2007).  $\theta$  in these regions is highly variable in space and time, where the physical, hydrologic and biotic characteristics of a given field site confer primary control of spatial variability in  $\theta$ . For example, patchiness of infiltration can lead to variations in vertical and horizontal patterns of  $\theta$ , nutrient redistribution, and biogeochemical weathering (Chorover et al., 2011). Similarly, temporal variations in  $\theta$  can be very strong in drylands, which experience pulses of precipitation interspersed by long dry periods (Huxman et al., 2004b; Schwinning and Sala, 2004; Morton et al., 2011). The dynamics of these pulses have an important impact on carbon assimilation by plants, which depend upon the amount, intermittency and magnitude of precipitation events (Porporato et al., 2004). The trigger–transfer–reserve–pulse framework was developed to characterise ecohydrologic responses to rainfall intermittency in semi-arid landscapes (Ludwig et al., 2005). In this framework, pulses of production by vegetation are triggered by pulses of precipitation that exceed a threshold for activity, which can be influenced by the amount of moisture already stored in the soil and by the transfer of water horizontally and vertically.

The water budget represents the balance between moisture input as precipitation ( $P$ ) and output as evapotranspiration ( $ET$ ), net runoff ( $Q$ , runoff – run-on), net drainage below the root zone ( $D$ , the difference between groundwater recharge and discharge) and the change in storage of  $\theta$  ( $\Delta\theta$ ):

$$P = ET + Q + D + \Delta\theta. \quad (1)$$

Much of the Australian drylands are covered by Mulga (*Acacia* spp.) shrubs and trees (30–35% of the semi-arid land area) (Bowman et al., 2008), and these Mulga lands tend to be flat with negligible runoff or drainage (Pressland, 1976a; Murphy et al., 2010; Moreno-de las Heras et al., 2012; Chen et al., 2014). Thus, slope and lithology alone explain 16% of Mulga distribution such that their density declines rapidly when the slope of the terrain increases above 2% (Murphy et al.,

2010). Furthermore, Mulga is distributed on water-storing substrates (sand dunes, clay-rich soils, and over hardpan) where drainage is limited or absent (Pressland, 1976a). As a potentially important source of water for maintaining physiological activity during dry seasons and droughts, the carry-over of stored soil moisture can influence phenology, productivity and ET (Flanagan and Adkinson, 2011; Chen et al., 2016). Vegetation patches enhance infiltration by creating preferential flow paths along live and recently deceased roots and by concentrating delivery of water from precipitation to the base of the tree via stemflow (Ludwig et al., 2005). Large proportions of precipitation (18–40%) are channelled as stemflow down the mostly vertical branches of Mulga, thereby concentrating the storage of soil moisture into a small area near the bole (Pressland, 1973, 1976b; Tongway and Ludwig, 1990). By concentrating rainfall to near the base of the trees,  $\theta$  in the inter-tree spaces tends to be small even following precipitation, except following large storms (e.g., when the single-storm precipitation is larger than 50 mm; Pressland, 1976a). Local capture of soil moisture by Mulga contributes to disruption of runoff at the landscape scale but enhances local redistribution of moisture from open spaces to underneath the trees (Dunkerley and Brown, 1995). In Mulga where soil moisture storage capacity is large, understanding pulse responses alone is insufficient for understanding ecosystem responses to precipitation (Lauenroth et al., 2014) because the reserve of soil moisture provides an important connection between a previous precipitation event and growth (Ludwig et al., 2005).

The presence of a hardpan is an important feature of many semi-arid environments, having the potential for affecting local (i.e., fine scale) distributions of moisture availability (Mohawesh et al., 2008). Various forms of siliceous (i.e., silica- or sand-based) hardpan underlie vast portions of the semi-arid regions of Australia (Litchfield and Mabbutt, 1962; Chartres, 1985), isolating the root zone from distant bedrock or groundwater in the locations where it occurs (Cleverly et al., 2016b). The physical characteristics of these hardpans have an important impact on the hydrology and ecology of the ecosystems where they occur. Siliceous hardpans form in dry sands containing traces of gypsum, opal and alunite (Thiry et al., 2006). However, these binding agents dissolve when soil is wetted, and the durability of the hardpan (i.e., resistance to dissolution and infiltration) is proportional to the clay content of the soil (Litchfield and Mabbutt, 1962; Chartres, 1985). Thus, hardpans do not form in drainage sands, but they can underlie sand plains and dunes, creating an impenetrable barrier of varying thickness and depth and promoting accumulation of soil moisture in the unconsolidated soil above the hardpan. Hardpans in the strongly weathered red earths (kandosols) of Australia can be deep (> 3 m to the top of the hardpan), but large areas of the continent exist over a shallow hardpan buried between 0.3 and 1 m below the surface (Morton et al., 2011). Because of this variation, siliceous hardpans could have a profound effect on local hydrology and  $\theta$ . In landscapes containing a hardpan barrier to drainage, the total capacity for storage of water above the hardpan as soil moisture is proportional to the depth of unconsolidated soil above the hardpan. Thus, variability in hardpan depth is likely to affect plant and root distribution, which will then reinforce spatial patterns in  $\theta$ . Consequently, Mulga density increases where depth to the top of the hardpan is large (Tongway and Ludwig, 1990), implying that Mulga density increases with soil moisture storage capacity above the

hardpan. In this study, we will only address the fine-scale, not regional, effects of the hardpan on the relationships amongst  $\theta$ , soil moisture storage, phenology and productivity.

Hydraulic redistribution by plant roots is found commonly in semi-arid regions, although it is not confined to drylands (Caldwell et al., 1998). With hydraulic redistribution (of which “hydraulic lift” represents upward hydraulic redistribution), moisture is passively transported via roots across water potential gradients in the soil that are larger than the soil–leaf gradient (Hultine et al., 2003a; Loik et al., 2004; Neumann and Cardon, 2012). Reduction of the soil–leaf gradient in water potential is dependent upon substantial reductions in stomatal conductance and transpiration (Caldwell et al., 1998; Hultine et al., 2003b, 2004; Prieto et al., 2010). Stomatal closure is known to occur at night (Caldwell and Richards, 1989; Hultine et al., 2003b), during the dormant season (Hultine et al., 2004) and during the day when atmospheric demand (i.e., vapour pressure deficit) is large (Zeppel et al., 2004; Neumann and Cardon, 2012), as is the case in Mulga during drier-than-average periods (Cleverly et al., 2013a; Eamus et al., 2013). Hydraulic redistribution (whether nocturnal, dormant season or during daytime) can prevent root shrinkage (thereby maintaining contact between root and soil), prevent loss of xylem conductivity and increase root longevity, even into the dry season (Bauerle et al., 2008; Scott et al., 2008; Prieto and Ryel, 2014). By maintaining root function during dry periods, some species have the potential to respond rapidly following precipitation events without having to develop new root tissue.

Photosynthetic production in Mulga woodlands is driven by phenological responses in leaf-level productivity, photosynthetic capacity and new leaf growth that are induced by pulses of precipitation, which is why the enhanced vegetation index (EVI) is closely related to gross primary production across Australian drylands (Ma et al., 2013). Using the normalised difference vegetation index (NDVI) from MODIS, Moreno-de las Heras et al. (2012) found greenness in undisturbed Mulga to lag behind rainfall by 0–10 days at a given site (i.e., a lag of zero to two 8-day scenes). Typically in ecosystems driven by precipitation pulses, a pulse in net ecosystem productivity (NEP) follows precipitation by several days if the threshold for activity has been met (Huxman et al., 2004b), although the time required for photosynthetic assimilation to initiate might be only one day, depending upon the plant species (Huxman et al., 2004a). NEP represents the integrated effects of phenology and productivity in all types of photosynthetic organisms that are present in the ecosystem, thus the timing and magnitude of a response in NEP could be shortened by differential responses to precipitation events amongst organisms. Because of the close relationships between phenology and physiology, Migliavacca et al. (2015) introduced the term *physiological phenology* to include the seasonal variation in plant- and ecosystem-scale physiology (e.g., NEP).

Located where soils have a large capacity for storage of water, and the storms to recharge  $\theta$  are large and infrequent, Mulga is distributed in the more productive parts of the landscape (Murphy et al., 2010), where carbon is sequestered over long periods in woody tissue and long-lived evergreen leaves/phyllodes (Morton et al., 2011). An example of Mulga's productiveness was the large responses of NEP and gross primary production in this Mulga woodland to precipitation in 2011 (Cleverly et al., 2013a; Eamus et al., 2013). Mulga rangelands were identified as one of the semi-arid ecosystems in Australia that together contributed a majority (57%) of the 2011 global land carbon sink anomaly (Cleverly et al., 2016a), which was an anomalous increase in terrestrial carbon uptake in response to precipitation extremes across the Southern Hemisphere and associated reductions in mean sea level (Boening et al., 2012; Fasullo et al., 2013) that impacted the global carbon cycle (Poulter et al., 2014). By contrast, during the drought year following 2011, the Mulga woodlands were carbon neutral (i.e.,  $\text{NEP} \approx 0$ ; Cleverly et al., 2013a).

In this study, we evaluated the vertical, horizontal and temporal relationships between soil moisture, leaf phenology and NEP in a semi-arid Mulga woodland of central Australia. The primary photosynthetic

organisms in this Mulga woodland are  $C_3$  trees, an understorey dominated by  $C_4$  grasses, and biological soil crusts. The objective of this study was to investigate relationships amongst soil moisture, NEP (i.e., ecosystem scale physiological phenology), and phenological responses to precipitation in the photosynthetic organisms comprising the ecosystem (i.e., trees, grasses and biological soil crusts). We compared measurements of leaf greenness, NEP,  $\theta$  and root distribution in a Mulga woodland to investigate their relationships to key factors of the local water budget: precipitation and storage of water in the soil ( $\Delta\theta$ ). These measurements were collected locally at a fine scale to test the following three hypotheses regarding the critical zone of this Mulga woodland:

1. Responses of NEP to precipitation (i.e., ecosystem-scale physiological phenology) were expected to be proportional to inter-seasonal carry-over of stored soil moisture above the top of the hardpan.
2. The responses of phenology in the component organisms (Mulga, understorey grasses and biological soil crust) were hypothesised to respond differently to precipitation such that soil crust was expected to respond immediately, whereas Mulga and understorey grasses were hypothesised to respond more slowly with the growth of new roots and leaves.
3. The rhizosphere was hypothesised to be restricted to the unconsolidated soil above the hardpan (i.e., root density was hypothesised to be significantly larger above the hardpan than in the top of the hardpan), which hypothetically forms a barrier for root growth and infiltration of water, thereby also restricting soil moisture storage pools to above the hardpan.

## 2. Methods

### 2.1. Study site

This study was conducted at the Alice Mulga SuperSite, a part of the OzFlux and Australian SuperSite networks. Complete descriptions of the vegetation and soils can be found in Eamus et al. (2013) and Cleverly et al. (2013b). Briefly, the site contains a high-density Mulga woodland (76% cover,  $8 \text{ m}^2 \text{ ha}^{-1}$  basal area, 0.2–0.9 leaf area index) consisting of *Acacia aneura* and *Acacia aptaneura* (Eamus et al., 2013; Cleverly et al., 2016b). The extensive but sparse canopy results in very little shading of the understorey or soil by the canopy, thus the woodland is not dense enough, nor is the 6.5 m tall canopy tall enough, for this ecosystem to be considered a forest. The physiological activity of a seasonal understorey of tussock grasses (annual and perennial,  $C_3$  and  $C_4$ , but largely  $C_4$ ), forbs and shrubs is conditional upon receipt of adequate rainfall. The site also contains an extensive ground cover of biological soil crust, which consists primarily of cyanobacteria as the photosynthetic component (Jameson, 2012).

The location of this site is near the northern limit for Mulga, which is not found where winter precipitation is lacking, as is the case in the tropical savannas to the north (Nix and Austin, 1973). This site receives 86% of annual precipitation during the monsoon season between November and April (Cleverly et al., 2013a), although this proportion varies inter-annually. The monsoon tropics of Australia are defined by receipt of at least 85% of annual precipitation in the monsoon season (Bowman et al., 2010), which places the site just within the monsoon tropics. Average annual precipitation was 312.3 mm for the period 1987–November 2015 (<http://www.bom.gov.au>), with a range of 25.1 mm in 1928 to 954.9 mm in 1974 (SILO patched point data, <https://www.longpaddock.qld.gov.au/silo/>; Table 1).

The soil is loamy sand with an extensive siliceous hardpan. All of our measurements were made near the top of the hardpan or in the unconsolidated soil above the hardpan. We have inferred from soil moisture measurements (i.e., siliceous hardpans are dry with unvarying  $\theta$ ) that the top of the hardpan varies spatially, from the surface (i.e., surface expression of the hardpan; Cleverly et al., 2013a) to more than 1 m deep,



**Table 1**  
Historical precipitation statistics.

Year	Precipitation (mm yr <sup>-1</sup> )
1900–2012	254*
1900–1969	231*
1970–2012	316*
Five wettest	
1974	955
2010	833
2000	743
1975	676
1904	555
Five driest	
1928	25
1961	70
1964	76
1965	77
1994	97

\* Median.

which was the maximal depth at which we could insert soil moisture sensors into the highly compacted soil. The depth to the bottom of the hardpan is unknown, but possibly much deeper than could be excavated (maximum of 2 m depth with the 1.5 t excavator to which we had access) in these hard, dense soils. Depth-to-groundwater is 49 m, and the site is located on the fringe of the regional aquifer where aquifer thickness is much smaller than 10 m ([www.lrm.nt.gov.au/\\_data/assets/pdf\\_file/0003/13863/TiTree\\_Basin\\_Groundwater.pdf](http://www.lrm.nt.gov.au/_data/assets/pdf_file/0003/13863/TiTree_Basin_Groundwater.pdf)). The groundwater is too deep to affect the vegetation or water budget, even in the absence of the hardpan. In a carbon isotope ratio study of water-use efficiency, we inferred that the presence of a hardpan served as a barrier to groundwater access by vegetation, regardless of the depth to groundwater (8 or 49 m deep; Cleverly et al., 2016b). Soil bulk density ranges from 0.9 to 2.1 g cm<sup>-3</sup> in unconsolidated soil and hardpan, respectively.

## 2.2. Eddy covariance

The eddy covariance method (Baldocchi et al., 1988) was used to measure NEP and sensible heat flux (H), the latter of which is indicative of partitioning of energy across seasons and years. Details on methods of measurements, quality control, corrections and gap filling can be found in Eamus et al. (2013) and Cleverly et al. (2013a). We will briefly summarise these methods here. These data are made available by the OzFlux network (Cleverly, 2011). Data processing was performed in the OzFluxQC Simulator, version 2.8.6 (Cleverly and Isaac, 2015), a summary of which follows.

NEP (mgCO<sub>2</sub> m<sup>-2</sup> s<sup>-1</sup>) and H (W m<sup>-2</sup>) were determined as the negative covariance between vertical wind speed (*w*) versus CO<sub>2</sub> density (*c*) or air temperature (*T*), respectively:

$$NEP = -\rho \langle w'c' \rangle \text{ and} \quad (2)$$

$$H = \rho C_p \langle w'T' \rangle. \quad (3)$$

where  $\rho$  and  $C_p$  are the density and heat capacity of moist air, respectively;  $w'$ ,  $c'$  and  $T'$  are the deviations from mean  $w$  and  $c$  and  $T$ , respectively; and  $\langle \rangle$  represents a time average. Measurements were collected at 10 Hz, and the averaging period was 30 min. Measurements were made at a height of 11.7 m over the homogeneous 6.5 m tall canopy. Wind speed measurements were made in three dimensions using a CSAT3 sonic anemometer (Campbell Scientific Australia, Townsville, QLD, Australia), and CO<sub>2</sub> density measurements were obtained from a LI7500 infrared gas analyser (IRGA, Li-Cor Biosciences, Lincoln, NE, USA). Ancillary measurements collected by the eddy covariance system were used in the subsequent quality control procedures and included

precipitation (CS7000, Hydrologic services, Warwick, NSW, Australia); temperature and relative humidity (HMP45C, Vaisala, Helsinki, Finland); and radiant fluxes in four components: upwelling and downwelling solar and thermal radiation (CNR1, Kipp and Zonen, Delft, The Netherlands). The system also included measurements of temperature and relative humidity (HMP45C) in a profile at heights of 2 m, 4.25 m (the zero-plane displacement height) and 6.5 m (the average canopy height) (Cleverly et al., 2013b).

### 2.2.1. Quality control, corrections and gap filling

Standard QC methods included spike detection using a standard deviation test, range checks for unrealistic values, identification of invalid measurements from CSAT and IRGA diagnostics, and identification of invalid IRGA measurements from outliers in the relationship between humidity measured by the HMP45C and IRGA. Corrections included double rotation, the Massman frequency response correction, conversion of virtual heat flux to sensible heat flux, and the Webb–Pearman–Leuning correction for flux effects on density measurements (Wesely, 1970; Webb et al., 1980; Massman and Clement, 2004). When there were no gaps in the ancillary measurements, gap filling of fluxes was performed using a self-organising linear output (SOLO) model, which is a type of artificial neural network (ANN) that produces small errors and has low sensitivity to overtraining, in contrast to feed-forward ANNs (Hsu et al., 2002; Eamus et al., 2013).

### 2.3. Phenocams and airborne imagery

Images of the vegetation (understorey grasses, Mulga canopy) and cryptobiotic crust were collected hourly during the daytime for evaluation of phenological activity. The cameras (5 Megapixel Wingscape timelapse, Wingscapes, AL, USA) were designed for repeat photography and configured to maintain a fixed white balance. The cameras were positioned at a 30° inclination and facing North to avoid backscattering during most of the year. Images that were obtained near solar noon were analysed for the green:red ratio index (GRRI), which provides an index of “greenness” that represents the trade-off between photosynthesis (due to chlorophyll content) and thermal dissipation (due to anthocyanin content) (Gamon and Surfus, 1999; Ritchie et al., 2010). Within each image, pixels were classified as Mulga, grass, crust or soil, after which GRRI was determined using Matlab (R2013a, The MathWorks Inc., Natick Massachusetts USA). Larger values of GRRI are indicative of enhanced physiological capacity. Because of technical issues with powering the cameras, analysis of phenology was restricted to a few precipitation events during key seasons.

Radiometric canopy temperature was measured to evaluate the thermal environment of the Mulga within the context of its photosynthetic thermal tolerances (i.e., 30 °C thermal optimum and 38 °C limit for photosynthesis and growth; Nix and Austin, 1973). Because the radiometric temperature of understorey and crust elements is indistinguishable from soil temperature due to their proximity to this large source of heat, this analysis was focused upon the canopy trees (i.e., Mulga). This analysis will determine if Mulga's thermal environment is conducive for maintenance of phyllode function. Aerial imagery was obtained on 27 March 2014 from an unmanned aerial vehicle (UAV), the AT8 octocopter of AerialTronics (Scheveningen, The Netherlands). Imagery was captured near mid-day to minimise shadow effects. The camera gimbal was set at a vertical angle (nadir-looking) during the flights. Two cameras were on board the UAV: a digital camera (red, green and blue; RGB) and a thermal camera. The thermal camera was a FLIR SC305 (FLIR Systems, Inc., Wilsonville, OR, USA) with a resolution of 320 × 240 pixels, a thermal accuracy of ± 2 °C, and a thermal sensitivity of 0.05 °C. The thermal field of view (FOV) was 45° × 34° (equipped with a 10 mm lens). All FLIR images were converted to canopy temperature tiff-images as described by Maes et al. (2014). Geo-referenced thermal and visual orthophotos were registered and co-registered manually in ArcGIS 10.1 (ESRI, Redlands, CA, USA).

## 2.4. Soil moisture and root profile characterisation

$\theta$  was measured in six arrays of vertical profiles. Sensors (CS616 and CS605) were buried at four depths: 0–10 cm (surface), 10–30 cm, 60–80 cm and 100–130 cm. These vertical profiles of  $\theta$  measurements were obtained from two arrays within each of three key habitats: under Mulga, in bare soil between trees, and beneath both Mulga and understorey. The latter habitat was identified during the build-up of the 2011 land carbon sink anomaly, when the understorey of grasses and herbs was present (Eamus et al., 2013). To avoid the confounding effects of transience of the understorey on patterns in  $\theta$ , we will present profiles from beneath the canopy and inter-canopy bare soil only. Calibration of the sensors, which is necessary to ensure accurate measurement of  $\theta$ , was performed by comparison to soil samples for laboratory analysis of soil texture, bulk density and  $\theta$  (Cleverly et al., 2013a).

Six trenches were dug about 1.2 km to the east of the tower in the Mulga woodland for evaluation of root density profiles with depth. Because of the large fetch of relatively homogenous vegetation at the tower (> 10 km in the predominant wind directions; Cleverly et al., 2013a), the location where the trenches were dug is representative of the ecosystem where continuous measurements of  $\theta$  were collected. Furthermore, flux footprints can extend this far under stable conditions at night (Göckede et al., 2008), further implying that this location is representative of the tower site to the west. Trenches were placed in three habitats: beneath Mulga near the bole (Mulga), in bare soil patches (bare soil) and below the edge of the projected canopy. Intact soil cores were collected for root extraction from the trench face at 25 cm intervals to a depth of 125 cm. Additional soil cores for analysis of bulk density and  $\theta$  were collected to identify the top of the hardpan. The hardpan varied spatially by habitat at the trench locations as it does in the soil moisture arrays at the tower. The top of the hardpan varied between 0 and 0.6 m deep, in contrast to the tower site where the top of the hardpan varied from the surface to more than 1 m deep. The Mulga were shorter and less dense where the trenches were dug, thus facilitating access for the excavator. Roots were extracted from soil samples using a hydro-pneumatic elutriation system, in which a soil and root sample is submerged in a vertical column of flowing water, whilst the sample is agitated with low-pressure air (Smucker et al., 1982). Hydro-pneumatic elutriation is the most reliable means to separate roots from soil. The null hypothesis that no differences in root density amongst sampling locations would be found was tested using a two-factor ANOVA (depth  $\times$  habitat,  $\alpha = 0.05$ ) followed by *post-hoc* multiple comparisons (Matlab R2013).

## 3. Results

### 3.1. Soil moisture control over phenological responses to precipitation

The balance between photosynthetic production and physiological stress is represented by the green:red ratio index (GRRI) of the vegetation, and this ratio varied by growth form and season in the current study (Fig. 1). During the spring and early summer, three surfaces (understorey grass, Mulga foliage and cryptobiotic crust) had distinct GRRI values, and the larger GRRI for the grasses indicated that grasses were more active than Mulga, and both were greener than the crust (Fig. 1a). Immediate but unsustained greening responses to precipitation during the spring and early summer were evident in all surface types. By autumn, the three surface types had similar spectral responses to rainfall (Fig. 1b). However, inferences cannot be drawn during the intervening period because of equipment failure at this remote location.

Whereas the response of NEP to rainfall was delayed in January–March 2014, there was an immediate increase in NEP during January 2015 (Fig. 2b). Striking differences in the pattern of precipitation were present between these two summers. During January 2014, the single largest storm delivered 105 mm precipitation over six consecutive

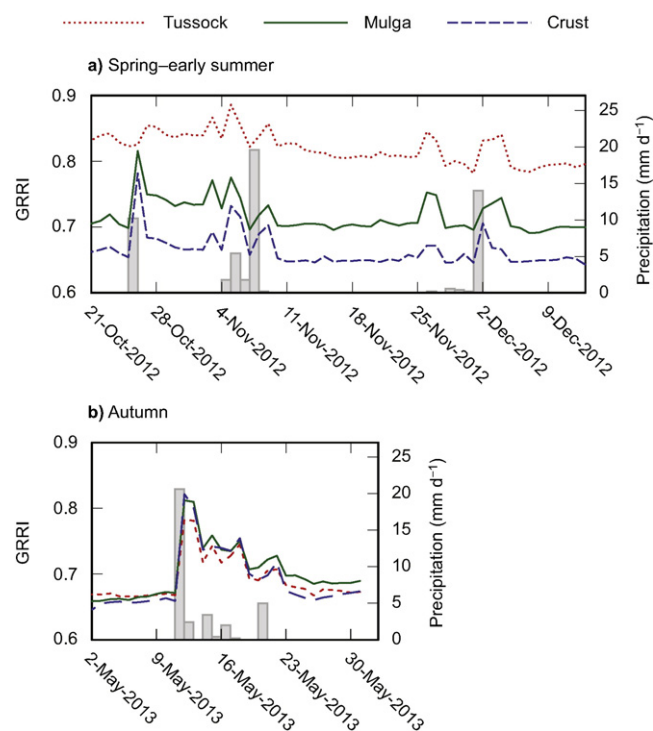


**Fig. 1.** Responses of the green:red ratio index (GRRI) to daily total precipitation (grey bars) in the tussock grass understorey (dotted line), Mulga foliage (solid line) and biological crust (dashed line) during (a) spring and early summer 2012 and (b) the following autumn 2013.

days. By contrast, 145 mm of precipitation fell over 12 consecutive days in January 2015. Even though each wet season received the same amount of precipitation, during the second year it was concentrated in December 2014 and January 2015 and was then followed by many months without substantial precipitation (Fig. 2b).

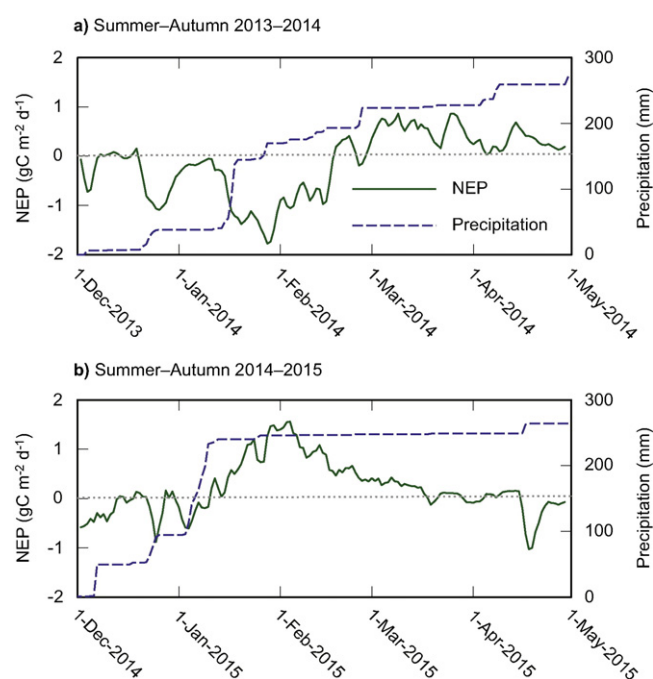


**Fig. 2.** Wet season dynamics of net ecosystem photosynthesis (NEP, three-day moving average, solid line) and cumulative precipitation (dashed line) during (a) Summer–Autumn 2013–2014 and (b) Summer–Autumn 2014–2015. Values of NEP larger than zero (horizontal dotted line) represent positive carbon uptake.

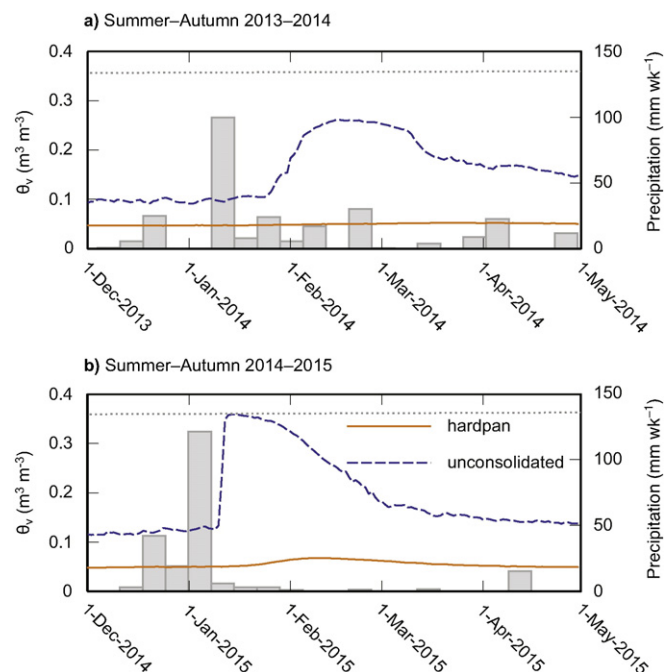


**Fig. 3.** Fluctuations of volumetric soil moisture content ( $\theta_v$ ) at 100 cm depth in hardpan (solid line) and unconsolidated loamy sand (dashed line). Soil porosity was  $0.35 \pm 0.006$  ( $n = 95$ , horizontal dotted line). Grey bars represent weekly total precipitation.

Differences in the pattern of precipitation during the wet season had a large effect on  $\theta$  of the root zone (Fig. 3). In Summer–Autumn 2013–2014,  $\theta$  in the unconsolidated soil above the hardpan increased to  $0.26 \text{ m}^3 \text{ m}^{-3}$  and remained at that level during the six week delay in NEP (cf. Figs. 2a and 3a), whereas  $\theta$  in the unconsolidated soil above the hardpan declined immediately during the next wet season (summer–autumn 2014–2015; Fig. 3b). Most of the year's precipitation was concentrated into a short period during December 2014–January 2015 (Figs. 2b and 3b), resulting in saturation of  $\theta$  in the unconsolidated soil above the hardpan at 1 m depth (Fig. 3b). Two-to-three weeks after saturation in the unconsolidated soil (mid-to-late January 2015),  $\theta$  in the hardpan at 1 m depth showed a slight increase, which was the first observed change in this very dry soil since measurements began in 2010.

Canopy temperature varied between a minimum of  $33^\circ\text{C}$  and a maximum of  $50^\circ\text{C}$ , although temperatures above  $ca. 46^\circ\text{C}$  were restricted to the edges of canopies (Fig. 4). Canopy temperatures were not uniformly distributed across the site, but it is difficult to identify a pattern in the clumped distribution of cool versus hot canopies. Canopy air temperature on the day of the thermal imagery was  $25.1^\circ\text{C}$  at 10.00,  $28.1^\circ\text{C}$  at 12.00 and reached a maximum of  $31.4^\circ\text{C}$  at 16.30. Thus, radiometric canopy temperatures were all above ambient air temperature, even after accounting for the  $\pm 2^\circ\text{C}$  precision of the thermal camera. Mid-day air temperatures tended to be lower in the seasons when NEP was large (autumn 2014 and summer 2015; cf. Table 2 and Fig. 2). Mid-day sensible heat flux was smallest during summer 2015, the wet season when NEP was large (cf. Table 2 and Fig. 2b). Sensible heat flux was equal in wet and dry seasons of 2014, although consistent

**Table 2**

Mid-day (10.00–14.00) air temperature measured at two metres height, sensible heat flux and average daily net ecosystem productivity (NEP) ( $\pm$  standard error). Days when precipitation occurred were not included.

Season	Period	Air temperature ( $^\circ\text{C}$ )	Sensible heat flux ( $\text{W m}^{-2}$ )	NEP ( $\text{gC m}^{-2} \text{ d}^{-1}$ )
Summer	21 January–10 February 2014	$34.1 \pm 0.2$	$307.1 \pm 6.7$	$-1.00 \pm 0.12$
Autumn	6–23 March 2014	$33.2 \pm 0.2$	$302.2 \pm 5.6$	$0.52 \pm 0.06$
Summer	21 January–10 February 2015	$33.5 \pm 0.2$	$270.4 \pm 5.4$	$1.23 \pm 0.07$
Autumn	6–23 March 2015	$34.0 \pm 0.3$	$367.3 \pm 5.3$	$0.23 \pm 0.04$

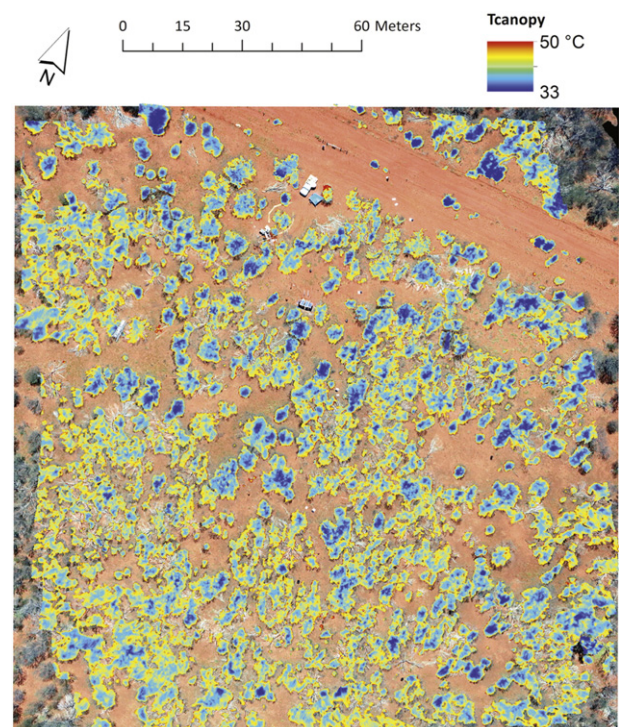


**Fig. 4.** Variability in thermal infrared canopy temperature measured from a low-altitude, unmanned aircraft (drone) on 27 March 2014.

season  $\times$  year relationships emerged. During summer 2014 (when NEP was delayed relative to precipitation), sensible heat flux was larger than during summer 2015 (when the response of NEP to precipitation was immediate; cf. Table 2 and Fig. 2b). Similarly, sensible heat flux in autumn 2014 (when NEP was large) was smaller than during autumn 2015 (when NEP was declining; cf. Table 2 and Fig. 2a).

The  $\theta$  profiles showed varied responses to precipitation (Fig. 5). Under dry conditions before summer rainfall,  $\theta$  at the surface was small in both habitats and smaller in bare soil ( $0.031 \pm 0.000074 \text{ m}^3 \text{ m}^{-3}$ ) than under Mulga ( $0.054 \pm 0.0012 \text{ m}^3 \text{ m}^{-3}$ ; Fig. 5). In response to a small autumnal storm (30 mm), moisture penetrated no deeper than 10 cm into the soil (Fig. 5a, b). By contrast, a large storm (100+ mm) produced widely varying soil moisture dynamics (Fig. 5c). The wetting front did not reach to 1 m depth in half of the profiles, whilst  $\theta$  was very large beneath Mulga where the  $\theta$  had been already large (i.e., in the consolidated soil above the hardpan; cf. Figs. 3a and 5c) and at one location beneath bare soil, implying that the durability of the hardpan against wetting was spatially variable.

### 3.2. Rhizosphere

Significant variation in root density was found within the woodland (depth  $\times$  habitat  $F = 6.09$ ;  $df = 10, 287$ ;  $p < 0.0001$ ). Substantial amounts of root biomass were observed only above 75 cm depth and directly beneath the base of Mulga trees. Root density in bare soil was not



significantly different from root density at the edge of the canopy, regardless of depth (Fig. 6). Root density was significantly larger near the boles of Mulga trees than in bare soil or under the edge of the canopy at depths of 5 and 50 cm (Fig. 6). The largest amounts of root biomass were located in the top 10 cm, although a secondary proliferation of root biomass above the top of hardpan (ca. 60 cm depth at the base of the trees) was also evident (Fig. 6).

Fig. 7 shows the daily soil moisture drawdown above the hardpan at 100 cm depth. During inter-storm periods,  $\theta$  above the hardpan at 100 cm depth began declining between 10:00 and 11:00 ( $0.11 \pm$

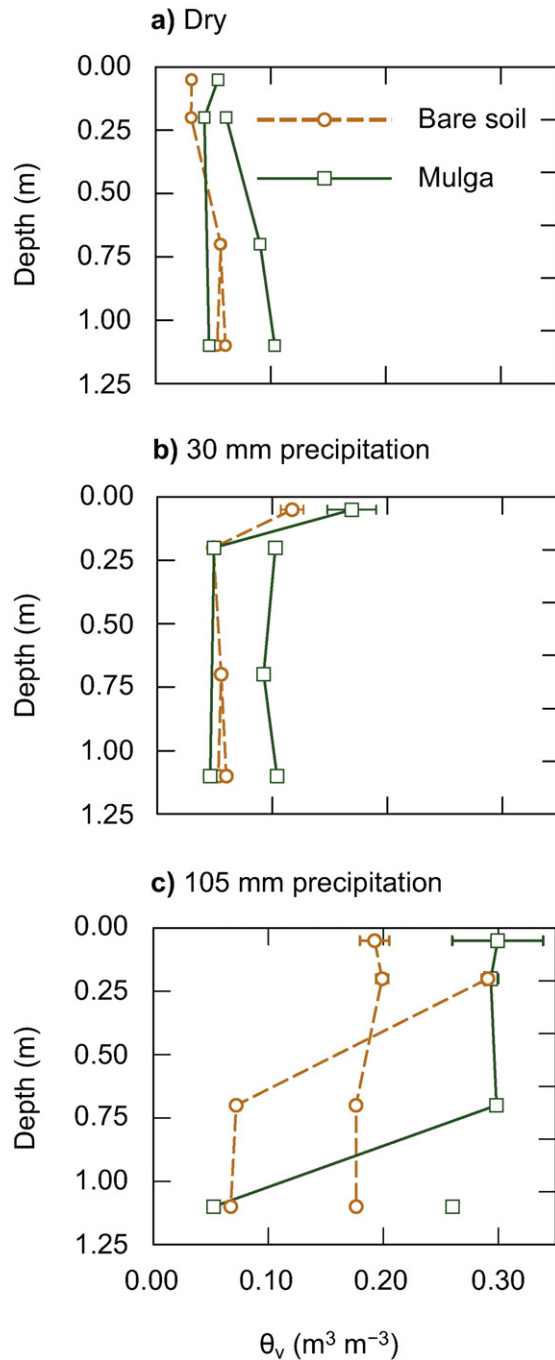


**Fig. 5.** Soil moisture profiles measured in replicate arrays beneath bare soil (circles and dashed line) and Mulga (squares and solid line) (a) before (2–11 May 2013) and during (b) a small storm (12–21 May 2013); or (c) during a large storm (15–24 January 2014). Symbols show mean  $\pm$  standard error. Lines connect measurements within the same sensor array. Values in (b, c) were computed as the average of the delayed peak response, if present. Missing values indicate sensors that were dysfunctional at the time of measurement.

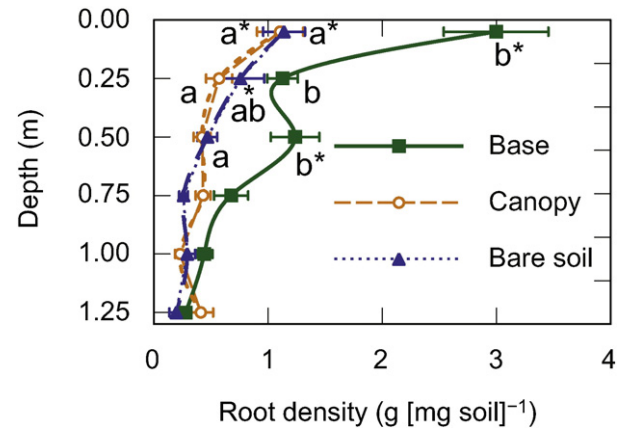


**Fig. 6.** Root density profile measured near the base of Mulga trees (squares and solid line), at the edge of the canopy (open circles and broken line), and in exposed hardpan (bare soil; triangles and dashed line). Symbols show mean  $\pm$  standard error ( $N = 294$ ). Symbols at the same depth with the same letter are not significantly different, and symbols marked with an asterisk are significantly different from the root density at 75 cm depth in the same habitat.

$0.00095 \text{ m}^3 \text{m}^{-3}$ ) and continued until reaching a minimum at 17:00 ( $0.083 \pm 0.0017 \text{ m}^3 \text{m}^{-3}$ ; Fig. 7). Recovery of  $\theta$  was rapid and reached the previous day's value before midnight (Fig. 7). In contrast during storms, diel variations in  $\theta$  above the hardpan at 100 cm depth were negligible (i.e., smaller than the measurement error; Fig. 7). The preceding soil moisture and rhizosphere results are summarised in Fig. 8.

## 4. Discussion

### 4.1. Triggers for photosynthetic responses

Reserves of soil moisture can serve as an important connection between precipitation and NEP (Ludwig et al., 2005; Flanagan and Adkinson, 2011). As we hypothesised, the storage of soil water provided inter-seasonal carry-over of available moisture, thereby supporting the enhancement of NEP during autumn 2014 (March 2014) after the conclusion of the wet season (Fig. 2a). By contrast, soil moisture carry-over did not occur during the wet season of a drier-than-average year (2012–2013,  $\theta$  ca.  $0.10 \text{ m}^3 \text{m}^{-3}$  in the unconsolidated soil above the hardpan), resulting in suppression of NEP through both summer and autumn

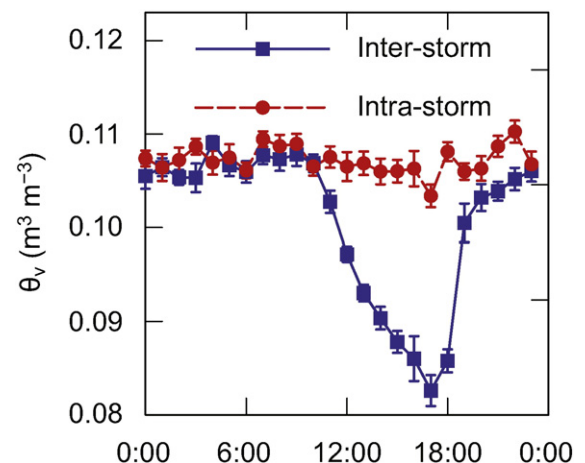


**Fig. 7.** Diel pattern of soil moisture content in unconsolidated soil, 100–120 cm depth, during inter-storm (5–8 February 2013, squares and solid line) and intra-storm (5.4 mm; 9–12 February 2013, circles and dashed line) periods. Symbols represent the mean  $\pm$  standard error for the four days.





factor was related to phenology in both types of vegetation, or the understorey grasses were facilitated by physiological activity in Mulga.

#### 4.2. Supporting the survival of a largely shallow root system

Mulga root systems are dimorphic, and we found them to be mostly restricted to above the hardpan in the unconsolidated soil as hypothesised, but the largest biomass was found near the surface (Fig. 5). The surface soil dries rapidly in this loamy sand (Eamus et al., 2013), thereby having a potentially detrimental effect on the roots located near the surface. A second and smaller proliferation of root biomass was located just above the top of the hardpan in the unconsolidated soil where storage of moisture accumulates.  $\theta$  in this store above the hardpan is drawn down by  $>0.02 \text{ m}^3 \text{ m}^{-3}$  on days without precipitation, although there are no discharge points for this soil moisture: evapotranspiration was at a minimum (Cleverly et al., 2016b), and drainage into the hardpan below was generally negligible. Furthermore, drawdown of  $\theta$  above the hardpan occurred during the hottest part of the day (Fig. 7), when Mulga are known to experience suppression of assimilation and stomatal conductance (Eamus et al., 2013) and when temperatures exceed the thermal tolerances for Mulga (Fig. 4; Cleverly et al., 2013a).

Stomatal closure in the presence of a split root system in which some roots are in dry soil and others are in wet soil presents the possibility of hydraulic lift (Bauerle et al., 2008). In this case, hydraulic redistribution would travel from roots in the soil moisture store above the hardpan to roots near the surface. Although we were unable to confirm the following reasoning with sapflux measurements, there are three lines of indirect evidence to support this hypothesis. First, the absence of discharge by evapotranspiration or drainage accounts for the other terms of the water budget; therefore, fluctuations in  $\theta$  were due to internal cycling (i.e., local changes in soil moisture storage). Second, we found a large proportion of the root biomass to occur near the surface where  $\theta$  is much smaller than at depth (Fig. 6), which is not unusual *per se*, except when encountered in dry soil (Caldwell et al., 1998). Third, synchronisation of tree and grass phenology after a delay in NEP further implies that the shallow-rooted tussock grasses obtain soil moisture as a result of moistening of the surface soil by hydraulic lift (Pugnaire et al., 1996; Ludwig et al., 2003), particularly in the absence of other soil moisture sources. During the delay period, high canopy temperature and unsaturated  $\theta$  kept the effects of hydraulic lift to a minimum, and precipitation alone was insufficient to sustain the understorey grasses. In the absence of other discharge points for soil moisture drawdown in the reservoir above the hardpan, it was most likely that hydraulic lift provided the connection between the synchronised phenology of individual photosynthetic organisms (trees, grasses and biological soil crust) and NEP.

Drawdown of  $\theta$  above the hardpan did not occur during storms, regardless of the amount of precipitation that was received. However, drawdown then resumed immediately upon the end of precipitation events (Fig. 7). This cessation of hydraulic lift is in contrast to a previous study on *Eucalyptus camaldulensis* and *Grevillea robusta* in which the seasonal return of rainfall initiated a reversal of hydraulic redistribution (i.e., translocation of soil moisture to deeper, drier soil layers; Burgess et al., 1998). There are two conditions during stormy periods that would tend to suppress, rather than reverse, hydraulic redistribution: (i) if precipitation wets the surface soils to equivalent  $\theta$  as in the soil moisture reserve, thereby eliminating or substantially reducing gradients in soil water potential (Hultine et al., 2003b); or (ii) if plant water status is much improved under small vapour pressure deficit during precipitation and cloud cover (Cleverly et al., 2013a; Page et al., 2016), resulting in small but non-negligible rates of stomatal conductance throughout the day. Thus, the water potential gradient during stormy conditions from any part of the root system to the air *via* stomata was much larger than water potential gradients across the root system, thereby eliminating the conditions favourable for hydraulic redistribution and resulting in cessation of daily fluctuations in  $\theta$ .

## 5. Conclusions

Covering 20–25% of Australia, Mulga woodlands are a potentially important part of continental carbon and water dynamics. The persistence and responsiveness of these woodlands can be understood through a detailed understanding of the critical zone, and particularly those attributes of the lithosphere, hydrosphere, biosphere and atmosphere that interact to drive constraints on the growth and productivity of vegetation. In north central Australia, the presence of siliceous hardpan can influence the spatial distribution of soil moisture reservoirs and roots within a few metres of the surface. These soil moisture reservoirs above the hardpan provide for the carry-over of soil moisture within the shallow rhizosphere of Mulga across seasons and years.

Carry-over of soil moisture can be a crucial resource for vegetation that experiences prolonged dry periods. In semi-arid regions, recharge of soil moisture reservoirs can be unpredictable, as can the duration between recharge events. It is common for precipitation to fail in central Australia, but the conservative use of soil moisture imposed by thermal stress on the canopy as the reservoir is drained ensures that carry-over persists beyond a single year. Even upon receiving large amounts of precipitation ( $100 \text{ mm wk}^{-1}$ ), the accumulation of soil moisture provides a buffer for delaying productivity until favourable conditions are present, when evaporation of that moisture contributes to preventing overheating of the canopy above Mulga's thermal limit.

Mulga has a dimorphic root distribution, with the majority of the root biomass in the top 10 cm of the soil and a second significant proliferation of roots just above the hardpan. During the long, dry periods between storms, the presence of hydraulic lift to the shallow roots was inferred from daily fluctuations in  $\theta$  above the hardpan, synchronisation of phenology amongst grasses and trees, and the absence of other discharge points (i.e., negligible drainage and evapotranspiration). We propose that through this mechanism, functioning of the shallow root system was maintained, which provided Mulga's roots and evergreen leaves with the capability of responding rapidly (i.e., if the conditions were favourable) to short, unpredictable, and large storms (i.e., with immediate moisture uptake through the roots to support immediate photosynthetic responses in the leaves). This resilience (i.e., physiological drought tolerance that does not diminish photosynthetic responses to subsequent wet periods) is the fundamental property that placed the Mulga lands of Australia in the heart of the 2011 global land carbon sink anomaly.

## Acknowledgements

This work was supported by grants from the Australian Government's Terrestrial Ecosystems Research Network (TERN) ([www.tern.gov.au](http://www.tern.gov.au)), the National Centre for Groundwater Research and Training (NCGRT), and the Australian Research Council (DP140101150). This work was supported also by OzFlux and the Australian Supersite Network, both parts of TERN and the latter of which is a research infrastructure facility established under the National Collaborative Research Infrastructure Strategy and Education Infrastructure Fund, Super Science Initiative, through the Department of Industry, Innovation, Science, Research and Tertiary Education. This research was also supported by a UTS re-establishment grant to "setup a phenocam network on key Australian ecosystems."

## References

- Baldocchi, D.D., Hicks, B.B., Meyers, T.P., 1988. Measuring biosphere-atmosphere exchanges of biologically related gases with micrometeorological methods. *Ecology* 69, 1331–1340.
- Ballhaus, C.G., Stumpf, E.F., 1985. Occurrence and petrological significance of graphite in the upper critical zone, Western Bushveld complex, South Africa. *Earth Planet. Sci. Lett.* 74, 58–68. [http://dx.doi.org/10.1016/0012-821x\(85\)90166-9](http://dx.doi.org/10.1016/0012-821x(85)90166-9).
- Banwart, S., Bernasconi, S.M., Bloem, J., Blum, W., Brandao, M., Brantley, S., Chabaux, F., Duffy, C., Kram, P., Lair, G., Lundin, L., Nikolaidis, N., Novak, M., Panagos, P., Ragnarsdottir, K.V., Reynolds, B., Rousseeva, S., de Ruiter, P., van Gaans, P., van

- Riemsdijk, W., White, T., Zhang, B., 2011. Soil processes and functions in critical zone observatories: hypotheses and experimental design. *Vadose Zone J.* 10, 974–987. <http://dx.doi.org/10.2136/vzj2010.0136>.
- Bauerle, T.L., Richards, J.H., Smart, D.R., Eissenstat, D.M., 2008. Importance of internal hydraulic redistribution for prolonging the lifespan of roots in dry soil. *Plant Cell Environ.* 31, 177–186. <http://dx.doi.org/10.1111/j.1365-3040.2007.01749.x>.
- Boening, C., Willis, J.K., Landerer, F.W., Nerem, R.S., Fasullo, J., 2012. The 2011 La Niña: so strong, the oceans fell. *Geophys. Res. Lett.* 39. <http://dx.doi.org/10.1029/2012gl053055>.
- Bowman, D., Boggs, G.S., Prior, L.D., 2008. Fire maintains an *Acacia aneura* shrubland–*Triodia* grassland mosaic in central Australia. *J. Arid Environ.* 72, 34–47. <http://dx.doi.org/10.1016/j.jaridenv.2007.04.001>.
- Bowman, D., Brown, G.K., Braby, M.F., Brown, J.R., Cook, L.G., Crisp, M.D., Ford, F., Haberle, S., Hughes, J., Isagi, Y., Joseph, L., McBride, J., Nelson, G., Ladiges, P.Y., 2010. Biogeography of the Australian monsoon tropics. *J. Biogeogr.* 37, 201–216. <http://dx.doi.org/10.1111/j.1365-2699.2009.02210.x>.
- Burgess, S.S.O., Adams, M.A., Turner, N.C., Ong, C.K., 1998. The redistribution of soil water by tree root systems. *Oecologia* 115, 306–311. <http://dx.doi.org/10.1007/s004420050521>.
- Caldwell, M.M., Richards, J.H., 1989. Hydraulic lift: water efflux from upper roots improves effectiveness of water uptake by deep roots. *Oecologia* 79, 1–5. <http://dx.doi.org/10.1007/bf00378231>.
- Caldwell, M.M., Dawson, T.E., Richards, J.H., 1998. Hydraulic lift: consequences of water efflux from the roots of plants. *Oecologia* 113, 151–161. <http://dx.doi.org/10.1007/s004420050363>.
- Chartres, C.J., 1985. A preliminary investigation of hardpan horizons in Northwest New South Wales. *Aust. J. Soil Res.* 23, 325–337. <http://dx.doi.org/10.1071/sr9850325>.
- Chen, C., Eamus, D., Cleverly, J., Boulain, N., Cook, P., Zhang, L., Cheng, L., Yu, Q., 2014. Modelling vegetation water-use and groundwater recharge as affected by climate variability in an arid-zone *Acacia* savanna woodland. *J. Hydrol.* 519, 1084–1096. <http://dx.doi.org/10.1016/j.jhydrol.2014.08.032>.
- Chen, C., Cleverly, J., Zhang, L., Yu, Q., Eamus, D., 2016. Modelling seasonal and inter-annual variations in carbon and water fluxes in an arid-zone *Acacia* savanna woodland, 1981–2012. *Ecosystems* 19, 625–644. <http://dx.doi.org/10.1007/s10021-015-9956-8>.
- Chorover, J., Troch, P.A., Rasmussen, C., Brooks, P.D., Pelletier, J.D., Breshears, D.D., Huxman, T.E., Kurc, S.A., Lohse, K.A., McIntosh, J.C., Meixner, T., Schaap, M.G., Litvak, M.E., Perdrill, J., Harpold, A., Durcik, M., 2011. How water, carbon, and energy drive critical zone evolution: the Jemez–Santa Catalina Critical Zone Observatory. *Vadose Zone J.* 10, 884–899. <http://dx.doi.org/10.2136/vzj2010.0132>.
- Cleverly, J., 2011. Alice Springs Mulga OzFlux site. Australian and New Zealand Flux Research and Monitoring Network. [OzFluxhdl.handle.net/102.100.100/8697](http://OzFluxhdl.handle.net/102.100.100/8697).
- Cleverly, J., Isaac, P., 2015. OzFluxQC Simulator version 2.8.6. GitHub repository <http://dx.doi.org/10.5281/zenodo.13730> (github.com/james-cleverly/OzFluxQC-Simulator).
- Cleverly, J., Boulain, N., Villalobos-Vega, R., Grant, N., Faux, R., Wood, C., Cook, P.G., Yu, Q., Leigh, A., Eamus, D., 2013a. Dynamics of component carbon fluxes in a semi-arid *Acacia* woodland, central Australia. *J. Geophys. Res. Biogeosci.* 118, 1168–1185. <http://dx.doi.org/10.1002/jgrg.20101>.
- Cleverly, J., Chen, C., Boulain, N., Villalobos-Vega, R., Faux, R., Grant, N., Yu, Q., Eamus, D., 2013b. Aerodynamic resistance and Penman–Monteith evapotranspiration over a seasonally two-layered canopy in semiarid central Australia. *J. Hydrometeorol.* 14, 1562–1570. <http://dx.doi.org/10.1175/jhm-d-13-080.1>.
- Cleverly, J., Thibault, J.R., Teet, S.B., Tashjian, P., Hipps, L.E., Dahm, C.N., Eamus, D., 2015. Flooding regime impacts on radiation, evapotranspiration and latent heat fluxes over groundwater-dependent riparian cottonwood and saltcedar forests. *Adv. Meteorol.* 2015, 935060. <http://dx.doi.org/10.1155/2015/935060>.
- Cleverly, J., Eamus, D., Luo, Q., Restrepo Coupe, N., Kijun, N., Ma, X., Ewen, C., Li, L., Yu, Q., Huete, A., 2016a. The importance of interacting climate modes on Australia's contribution to global carbon cycle extremes. *Sci. Rep.* 6, 23113. <http://dx.doi.org/10.1038/srep23113>.
- Cleverly, J., Eamus, D., Van Gorsel, E., Chen, C., Rumman, R., Luo, Q., Restrepo Coupe, N., Li, L., Kijun, N., Faux, R., Yu, Q., Huete, A., 2016b. Productivity and evapotranspiration of two contrasting semiarid ecosystems following the 2011 global carbon land sink anomaly. *Agric. For. Meteorol.* 220, 151–159. <http://dx.doi.org/10.1016/j.agrformet.2016.01.086>.
- Daudet, F.A., Le Roux, X., Sinoquet, H., Adam, B., 1999. Wind speed and leaf boundary layer conductance variation within tree crown—consequences on leaf-to-atmosphere coupling and tree functions. *Agric. For. Meteorol.* 97, 171–185. [http://dx.doi.org/10.1016/S0168-1923\(99\)00079-9](http://dx.doi.org/10.1016/S0168-1923(99)00079-9).
- Dunkerley, D.L., Brown, K.J., 1995. Runoff and runoff areas in a patterned chenopod shrubland, arid western New South Wales, Australia—characteristics and origin. *J. Arid Environ.* 30, 41–55.
- Eamus, D., Cleverly, J., Boulain, N., Grant, N., Faux, R., Villalobos-Vega, R., 2013. Carbon and water fluxes in an arid-zone *Acacia* savanna woodland: an analyses of seasonal patterns and responses to rainfall events. *Agric. For. Meteorol.* 182–183, 225–238. <http://dx.doi.org/10.1016/j.agrformet.2013.04.020>.
- Ehleringer, J.R., Monson, R.K., 1993. Evolutionary and ecological aspects of photosynthetic pathway variation. *Annu. Rev. Ecol. Syst.* 24, 411–439.
- Ehleringer, J.R., Sage, R.F., Flanagan, L.B., Pearcy, R.W., 1991. Climate change and the evolution of  $C_4$  photosynthesis. *Trends Ecol. Evol.* 6, 95–99. [http://dx.doi.org/10.1016/0169-5347\(91\)90183-x](http://dx.doi.org/10.1016/0169-5347(91)90183-x).
- Fasullo, J.T., Boening, C., Landerer, F.W., Nerem, R.S., 2013. Australia's unique influence on global sea level in 2010–2011. *Geophys. Res. Lett.* 40, 4368–4373. <http://dx.doi.org/10.1002/grl.50834>.
- Flanagan, L.B., Adkinson, A.C., 2011. Interacting controls on productivity in a northern Great Plains grassland and implications for response to ENSO events. *Glob. Chang. Biol.* 17, 3293–3311. <http://dx.doi.org/10.1111/j.1365-2486.2011.02461.x>.
- Gamon, J.A., Surfus, J.S., 1999. Assessing leaf pigment content and activity with a reflectometer. *New Phytol.* 143, 105–117. <http://dx.doi.org/10.1046/j.1469-8137.1999.00424.x>.
- Göckede, M., Foken, T., Aubinet, M., Aurela, M., Banza, J., Bernhofer, C., Bonnefond, J.M., Brunet, Y., Carrara, A., Clement, R., Dellwik, E., Elbers, J., Eugster, W., Fuhrer, J., Granier, A., Grunwald, T., Heinesch, B., Janssens, I.A., Knohl, A., Koeble, R., Laurila, T., Longdoz, B., Manca, G., Marek, M., Markkanen, T., Mateus, J., Matteucci, G., Mauder, M., Migliavacca, M., Minerbi, S., Moncrieff, J., Montagnani, L., Moors, E., Ourcival, J.M., Papale, D., Pereira, J., Pilegaard, K., Pita, G., Rambal, S., Rebmann, C., Rodrigues, A., Rotenberg, E., Sanz, M.J., Sedlak, P., Seufert, G., Siebicke, L., Soussana, J.F., Valentini, R., Vesala, T., Verbeeck, H., Yakir, D., 2008. Quality control of CarboEurope flux data—Part 1: Coupling footprint analyses with flux data quality assessment to evaluate sites in forest ecosystems. *Biogeosciences* 5, 433–450.
- Grote, E.E., Belpap, J., Housman, D.C., Sparks, J.P., 2010. Carbon exchange in biological soil crust communities under differential temperatures and soil water contents: implications for global change. *Glob. Chang. Biol.* 16, 2763–2774. <http://dx.doi.org/10.1111/j.1365-2486.2010.02201.x>.
- Hsu, K.-I., Gupta, H.V., Gao, X., Sorooshian, S., Imam, B., 2002. Self-organizing linear output map (SOL) an artificial neural network suitable for hydrologic modeling and analysis. *Water Resour. Res.* 38, 1302. <http://dx.doi.org/10.1029/2001wr000795>.
- Hultine, K., Cable, W., Burgess, S., Williams, D., 2003a. Hydraulic redistribution by deep roots of a Chihuahuan Desert phreatophyte. *Tree Physiol.* 23, 353–360.
- Hultine, K.R., Williams, D.G., Burgess, S.S.O., Keefer, T.O., 2003b. Contrasting patterns of hydraulic redistribution in three desert phreatophytes. *Oecologia* 135, 167–175.
- Hultine, K.R., Scott, R.L., Cable, W.L., Goodrich, D.C., Williams, D.G., 2004. Hydraulic redistribution by a dominant, warm-desert phreatophyte: seasonal patterns and response to precipitation pulses. *Funct. Ecol.* 18, 530–538. <http://dx.doi.org/10.1111/j.0269-8463.2004.00867.x>.
- Huxman, T.E., Cable, J.M., Ignace, D.D., Eilts, J.A., English, N.B., Weltzin, J., Williams, D.G., 2004a. Response of net ecosystem gas exchange to a simulated precipitation pulse in a semi-arid grassland: the role of native versus non-native grasses and soil texture. *Oecologia* 141, 295–305. <http://dx.doi.org/10.1007/s00442-003-1389-y>.
- Huxman, T.E., Snyder, K.A., Tissue, D., Leffler, A.J., Ogle, K., Pockman, W.T., Sandquist, D.R., Potts, D.L., Schwinning, S., 2004b. Precipitation pulses and carbon fluxes in semiarid and arid ecosystems. *Oecologia* 141, 254–268. <http://dx.doi.org/10.1007/s00442-004-1682-4>.
- Jameson, J., 2012. *The importance of biological soil crust in Australian semi-arid ecosystems*. B.Sc. (Honours). University of Technology, Sydney, Sydney, NSW, Australia.
- Lauenroth, W.K., Schlaepfer, D.R., Bradford, J.B., 2014. Ecohydrology of dry regions: storage versus pulse soil water dynamics. *Ecosystems* 17, 1469–1479. <http://dx.doi.org/10.1007/s10021-014-9808-y>.
- Lin, H., 2010. Earth's critical zone and hydrogeology: concepts, characteristics, and advances. *Hydrol. Earth Syst. Sci.* 14, 25–45.
- Lin, H., 2011. Three principles of soil change and pedogenesis in time and space. *Soil Sci. Soc. Am. J.* 75, 2049–2070. <http://dx.doi.org/10.2136/sssaj2011.0130>.
- Litchfield, W.H., Mabbitt, J.A., 1962. Hardpan in soils of semi-arid Western Australia. *J. Soil Sci.* 13, 148–159.
- Loik, M.E., Breshears, D.D., Lauenroth, W.K., Belpap, J., 2004. A multi-scale perspective of water pulses in dryland ecosystems: climatology and ecohydrology of the western USA. *Oecologia* 141, 269–281.
- Ludwig, F., Dawson, T.E., de Kroon, H., Berendse, F., Prins, H.H.T., 2003. Hydraulic lift in *Acacia tortilis* trees on an East African savanna. *Oecologia* 134, 293–300. <http://dx.doi.org/10.1007/s00442-002-1119-x>.
- Ludwig, J.A., Wilcox, B.P., Breshears, D.D., Tongway, D.J., Imeson, A.C., 2005. Vegetation patches and runoff-erosion as interacting ecohydrological processes in semiarid landscapes. *Ecology* 86, 288–297.
- Ma, X., Huete, A., Yu, Q., Restrepo Coupe, N., Davies, K., Broich, M., Ratana, P., Beringer, J., Hutley, L.B., Cleverly, J., Boulain, N., Eamus, D., 2013. Spatial patterns and temporal dynamics in savanna vegetation phenology across the North Australian Tropical Transect. *Remote Sens. Environ.* 139, 97–115. <http://dx.doi.org/10.1016/j.rse.2013.07.030>.
- Maes, W.H., Minchin, P.E.H., Snelgar, W.P., Steppe, K., 2014. Early detection of *Psa* infection in kiwifruit by means of infrared thermography at leaf and orchard scale. *Funct. Plant Biol.* 41, 1207–1220. <http://dx.doi.org/10.1071/fp14021>.
- Martin, H.A., 2006. Cenozoic climatic change and the development of the arid vegetation in Australia. *J. Arid Environ.* 66, 533–563. <http://dx.doi.org/10.1016/j.jaridenv.2006.01.009>.
- Massman, W., Clement, R., 2004. Uncertainty in eddy covariance flux estimates resulting from spectral attenuation. In: Lee, X., Massman, W., Law, B. (Eds.), *Handbook of Micrometeorology: A Guide for Surface Flux Measurement and Analysis*. Kluwer Academic Publishers, Dordrecht/Boston/London, pp. 67–100.
- Migliavacca, M., Reichstein, M., Richardson, A.D., Mahecha, M.D., Cremonese, E., Delpierre, N., Galvagno, M., Law, B.E., Wohlfahrt, G., Black, T.A., Carvalhais, N., Ceccherini, G., Chen, J.Q., Gobron, N., Koffi, E., Munger, J.W., Perez-Priego, O., Robustelli, M., Tomelleri, E., Cescatti, A., 2015. Influence of physiological phenology on the seasonal pattern of ecosystem respiration in deciduous forests. *Glob. Chang. Biol.* 21, 363–376. <http://dx.doi.org/10.1111/gcb.12671>.
- Mohawesh, O., Ishida, T., Fukumura, K., Yoshino, K., 2008. Assessment of spatial variability of penetration resistance and hardpan characteristics in a cassava field. *Aust. J. Soil Res.* 46, 210–218. <http://dx.doi.org/10.1071/sr07118>.
- Moreno-de las Heras, M., Saco, P.M., Willgoose, G.R., Tongway, D.J., 2012. Variations in hydrological connectivity of Australian semiarid landscapes indicate abrupt changes in rainfall-use efficiency of vegetation. *J. Geophys. Res.* 117, G03009. <http://dx.doi.org/10.1029/2011jg001839>.
- Morton, S.R., Smith, D.M.S., Dickman, C.R., Dunkerley, D.L., Friedel, M.H., McAllister, R.R.J., Reid, J.R.W., Roshier, D.A., Smith, M.A., Walsh, F.J., Wardle, G.M., Watson, I.W.,

- Westoby, M., 2011. A fresh framework for the ecology of arid Australia. *J. Arid Environ.* 75, 313–329. <http://dx.doi.org/10.1016/j.jaridenv.2010.11.001>.
- Murphy, B.P., Paron, P., Prior, L.D., Boggs, G.S., Franklin, D.C., Bowman, D., 2010. Using generalized autoregressive error models to understand fire-vegetation-soil feedbacks in a mulga-spinifex landscape mosaic. *J. Biogeogr.* 37, 2169–2182. <http://dx.doi.org/10.1111/j.1365-2699.2010.02359.x>.
- Neumann, R.B., Cardon, Z.G., 2012. The magnitude of hydraulic redistribution by plant roots: a review and synthesis of empirical and modeling studies. *New Phytol.* 194, 337–352. <http://dx.doi.org/10.1111/j.1469-8137.2012.04088.x>.
- Nix, H.A., Austin, M.P., 1973. Mulga: a bioclimatic analysis. *Tropical Grasslands* 7, 9–20.
- Ogle, K., Reynolds, J.F., 2004. Plant responses to precipitation in desert ecosystems: integrating functional types, pulses, thresholds, and delays. *Oecologia* 141, 282–294. <http://dx.doi.org/10.1007/s00442-004-1507-5>.
- Page, G.F.M., Merchant, A., Grierson, P.E., 2016. Inter-specific differences in the dynamics of water use and pulse-response of co-dominant canopy species in a dryland woodland. *J. Arid Environ.* 124, 332–340. <http://dx.doi.org/10.1016/j.jaridenv.2015.09.004>.
- Porporato, A., Daly, E., Rodriguez-Iturbe, I., 2004. Soil water balance and ecosystem response to climate change. *Am. Nat.* 164, 625–632. <http://dx.doi.org/10.1086/424970>.
- Poulter, B., Frank, D., Ciais, P., Myneni, R.B., Andela, N., Bi, J., Broquet, G., Canadell, J.G., Chevallier, F., Liu, Y.Y., Running, S.W., Sitch, S., van der Werf, G.R., 2014. Contribution of semi-arid ecosystems to interannual variability of the global carbon cycle. *Nature* 509, 600–603. <http://dx.doi.org/10.1038/nature13376>.
- Pressland, A.J., 1973. Rainfall partitioning by an arid woodland (*Acacia aneura* F. Muell) in south-western Queensland. *Aust. J. Bot.* 21, 235–245. <http://dx.doi.org/10.1071/bt9730235>.
- Pressland, A.J., 1976a. Effect of stand density on water-use of mulga (*Acacia aneura* F. Muell) woodlands in southwestern Queensland. *Aust. J. Bot.* 24, 177–191. <http://dx.doi.org/10.1071/bt9760177>.
- Pressland, A.J., 1976b. Soil moisture redistribution as affected by throughfall and stemflow in an arid zone shrub community. *Aust. J. Bot.* 24, 641–649. <http://dx.doi.org/10.1071/bt9760641>.
- Prieto, I., Ryel, R.J., 2014. Internal hydraulic redistribution prevents the loss of root conductivity during drought. *Tree Physiol.* 34, 39–48. <http://dx.doi.org/10.1093/treephys/tpt115>.
- Prieto, I., Martinez-Tilleria, K., Martinez-Manchego, L., Montecinos, S., Pugnaire, F.I., Squeo, F.A., 2010. Hydraulic lift through transpiration suppression in shrubs from two arid ecosystems: patterns and control mechanisms. *Oecologia* 163, 855–865. <http://dx.doi.org/10.1007/s00442-010-1615-3>.
- Pugnaire, F.I., Haase, P., Puigdefabregas, J., 1996. Facilitation between higher plant species in a semiarid environment. *Ecology* 77, 1420–1426. <http://dx.doi.org/10.2307/2265539>.
- Reynolds, J.F., Stafford Smith, D.M., Lambin, E.F., Turner, B.L., Mortimore, M., Batterbury, S.P.J., Downing, T.E., Dowlatabadi, H., Fernandez, R.J., Herrick, J.E., Huber-Sannwald, E., Jiang, H., Leemans, R., Lynam, T., Maestre, F.T., Ayarza, M., Walker, B., 2007. Global desertification: Building a science for dryland development. *Science* 316, 847–851. <http://dx.doi.org/10.1126/science.1131634>.
- Ritchie, G.L., Sullivan, D.G., Vencill, W.K., Bednarz, C.W., Hook, J.E., 2010. Sensitivities of Normalized Difference Vegetation Index and a green/red ratio index to cotton ground cover fraction. *Crop Sci.* 50, 1000–1010. <http://dx.doi.org/10.2135/cropsci2009.04.0203>.
- Ryan, P.R., Delhaize, E., Jones, D.L., 2001. Function and mechanism of organic anion exudation from plant roots. *Annu. Rev. Plant Physiol. Plant Mol. Biol.* 52, 527–560. <http://dx.doi.org/10.1146/annurev.arplant.52.1.527>.
- Schuepp, P.H., 1993. Tansley review no. 59 Leaf boundary-layers. *New Phytol.* 125, 477–507. <http://dx.doi.org/10.1111/j.1469-8137.1993.tb03898.x>.
- Schwinning, S., Sala, O.E., 2004. Hierarchy of responses to resource pulses in arid and semi-arid ecosystems. *Oecologia* 141, 211–220. <http://dx.doi.org/10.1007/s00442-004-1520-8>.
- Scott, R.L., Cable, W.L., Hultine, K.R., 2008. The ecohydrologic significance of hydraulic redistribution in a semiarid savanna. *Water Resour. Res.* 44, W02440.
- Smucker, A.J.M., McBurney, S.L., Srivastava, A.K., 1982. Quantitative separation of roots from compacted soil profiles by the hydropneumatic elutriation system. *Agron. J.* 74, 500–503.
- Stevens, R.M., Ewenz, C.M., Grigson, G., Conner, S.M., 2012. Water use by an irrigated almond orchard. *Irrig. Sci.* 30, 189–200. <http://dx.doi.org/10.1007/s00271-011-0270-8>.
- Thiry, M., Milnes, A.R., Rayot, V., Simon-Coincon, R., 2006. Interpretation of palaeoweathering features and successive silicifications in the Tertiary regolith of inland Australia. *J. Geol. Soc.* 163, 723–736. <http://dx.doi.org/10.1144/0014-764905-020>.
- Tongway, D.J., Ludwig, J.A., 1990. Vegetation and soil patterning in semiarid mulga lands of Eastern Australia. *Aust. J. Ecol.* 15, 23–34. <http://dx.doi.org/10.1111/j.1442-9993.1990.tb01017.x>.
- Touboul, P., Saoudi, N., Atallah, G., Kirkorian, G., 1992. Catheter ablation for atrial-flutter: current concepts and results. *J. Cardiovasc. Electrophysiol.* 3, 641–652.
- Tsakalotos, D.E., 1909. The inner friction of the critical zone. *Z. Phys. Chem.-Stoch. Ve.* 68, 32–38.
- Webb, E., Pearman, G., Leuning, R., 1980. Correction of flux measurements for density effects due to heat and water-vapor transfer. *Q. J. R. Meteorol. Soc.* 106, 85–100.
- Wesely, M.L., 1970. Eddy Correlation Measurements in the Atmospheric Surface Layer Over Agricultural Crops Ph.D. Dissertation University of Wisconsin, Madison.
- Yunusa, I.A.M., Walker, R.R., Lu, P., 2004. Evapotranspiration components from energy balance, sapflow and microlysimetry techniques for an irrigated vineyard in inland Australia. *Agric. For. Meteorol.* 127, 93–107. <http://dx.doi.org/10.1016/j.agrformet.2004.07.001>.
- Zeppel, M.J.B., Murray, B.R., Barton, C., Eamus, D., 2004. Seasonal responses of xylem sap velocity to VPD and solar radiation during drought in a stand of native trees in temperate Australia. *Funct. Plant Biol.* 31, 461–470. <http://dx.doi.org/10.1071/fp03220>.